Available online at www.sciencedirect.com

Journal of Applied Research and Technology

Journal of Applied Research and Technology 14 (2016) 54–61

www.jart.ccadet.unam.mx

Original

Microstructure of polyacrylonitrile-based activated carbon fibers prepared from solvent-free coagulation process

Norhaniza Yusof[a,b,*], Dipak Rana[c], Ahmad Fauzi Ismail[a,b], Takeshi Matsuura[c]

[a] *Advanced Membrane Technology Research Centre (AMTEC), Universiti Teknologi Malaysia, 81310 Skudai, Johor Bahru, Malaysia*

[b] *Faculty of Chemical and Energy Engineering, Universiti Teknologi Malaysia, 81310 Skudai, Johor Bahru, Malaysia*

[c] *Department of Chemical and Biological Engineering, Industrial Membrane Research Institute, University of Ottawa, 161 Louis Pasteur Street, Ontario K1N 6N5, Canada*

Received 20 August 2015; accepted 4 February 2016

Available online 28 February 2016

Abstract

Polyacrylonitrile precursor fibers prepared using a solvent-free coagulation process were stabilized, carbonized, and physically activated by carbon dioxide into activated carbon fibers (ACFs). The activation temperature varied from 600 to 900 °C while the activation time was 1 h. Atomic force microscopy was used to observe the surface morphology, as well as the surface roughness of the ACFs. Higher pyrolysis temperature formed rougher surfaces, and increased the pore sizes. Meanwhile, Fourier transform infrared spectroscopy revealed more conversion of oxygen containing functional groups to carbonaceous materials as the activation temperature increased. Moreover, the microstructure properties were thoroughly characterized by the X-ray photoelectron spectroscopy (XPS) and X-ray diffraction (XRD) studies. XRD analysis showed that the activation of the ACFs shrank the ordered structure, reducing the D-spacing from 0.358 to 0.347 nm for the fibers prepared at activation temperatures of 600 to 900 °C. Meanwhile, XPS analysis concluded that that the oxygen containing functional groups were still retained even at high activation temperatures while the nitrogen containing functional groups were reduced during the high temperature activation in the CO_2 atmosphere.

Keywords: Activated carbon fibers; Solvent-free coagulation process; Physical activation; Microstructure

1. Introduction

Activated carbon fibers (ACFs) can be prepared from various precursors namely polyacrylonitrile (PAN), coal, rayon, phenolic resins and pitches (Tsai, 1994). Different precursors will give different properties of ACFs and the pore texture of the ACFs significantly depends on the nature of the precursors (Chiang, Lee, & Lee, 2007). Among ACFs based on many different precursors, PAN based ACFs have attracted much attention of many researchers due to its high adsorption performance when compared to other counterparts. However, the organic solvents such as dimethylformamide (DMF) and dimethylacetamide (DMAc), which were often employed in the conventional coagulation bath in the fabrication of PAN fibers, could cause cancer after a long period of exposure due to its carcinogenic effects (Ismail, Rahman, Mustafa, & Matsuura, 2008; Yusof & Ismail, 2012a; Yusof, Ismail, Rana, & Matsuura, 2012). Therefore, in an attempt to reduce the hazardous effects, we investigated the properties of PAN/acrylamide (AM) fiber using a solvent-free coagulation bath in hollow fiber spinning of the polymer dope. It is known that the micro-structure of the ACFs finally obtained depends not only on the nature of the precursor but also on the conditions of activation that follows the precursor hollow fiber spinning, such as the activation temperature and the activation time (Sedghi, Farsani, & Shokuhfar, 2008). Nevertheless, there have been no detailed studies until now to know how the activation procedure affects the surface structure of PAN-based ACFs, particularly when the precursor PAN hollow fibers are spun in the solvent-free coagulation bath. It should be noted that the presence of pores on the rayon-based ACFs surface was recently confirmed using AFM (Wang et al., 2011; Zhao, He,

* Corresponding author.
E-mail address: norhaniza@petroleum.utm.my (N. Yusof).
Peer Review under the responsibility of Universidad Nacional Autónoma de México.

http://dx.doi.org/10.1016/j.jart.2016.02.001

Jiang, Li, & Li, 2007). It seems therefore very interesting to apply the AFM and other characterization methods to investigate the effect of activation conditions on the surface structures of the newly developed ACFs.

Therefore, the objectives of this study are to investigate the manipulation of the activation temperature toward the enhancement of micro porous structure of PAN/AM-based activated carbon fibers prepared using a solvent-free coagulation bath. In pursuit of this goal, the fibers were extensively characterized by means of atomic force microscopy (AFM), Fourier transform infrared (FTIR) spectroscopy, wide angle X-ray diffraction (XRD), and X-ray photoelectron spectroscopy (XPS). With the aid of these analysis methods, it is expected that this will be helpful for us to understand the relationship between the morphological behavior and chemical structure of PAN-ACFs prepared by different activation conditions. The results obtained from this study were also compared to the trends reported by previous studies.

2. Experimental

2.1. Materials and fabrication of PAN fibers

Polyacrylonitrile (PAN) in powder form was obtained from Aldrich, USA. Meanwhile, acrylamide (AM) purchased from Sigma–Aldrich, Germany was used as an additive. Dimethylformamide (DMF) purchased from Merck, Germany was employed as the solvent. The method to prepare uniform spinning dope of PAN and AM in DMF was reported earlier (Ismail et al., 2008; Yusof & Ismail, 2012a; Yusof et al., 2012). Eighteen weight percent of PAN/DMF solution was prepared, into which 5% of AM was added. The slurry was heated continuously at 70 °C until a highly viscous dope solution became ready for the spinning process. Then, the homogeneous dope was degassed in an ultrasonic bath (Branson Ultrasonics) for 24 h to remove the gas bubbles present in the dope. The dry-jet-wet spinning technique was used to produce PAN fibers. The high interest regarding environmental issues has resulted in the development of PAN fiber fabrication in a solvent-free coagulation process using 100% tap water in the coagulation bath (Ismail et al., 2008; Yusof & Ismail, 2012a; Yusof et al., 2012). The spinning conditions used in this study are listed elsewhere (Yusof & Ismail, 2012a). The AM/PAN fibers have a round shape cross-section with a fiber diameter around 100 μm.

2.2. Pyrolysis process

The stabilization process was carried out under tension in an air flow condition by heating at a rate of 2 °C/min until 275 °C, before constant heating carried on for 30 min. This is an important step in preparing the fibers so that they can withstand higher temperatures without decomposing during the carbonization treatment by further orienting and then cross-linking the molecules (Sedghi et al., 2008; Yusof & Ismail, 2012b). The quality of the resulting activated carbon fibers depends strongly upon the degree of stabilization (Yusof & Ismail, 2012b).

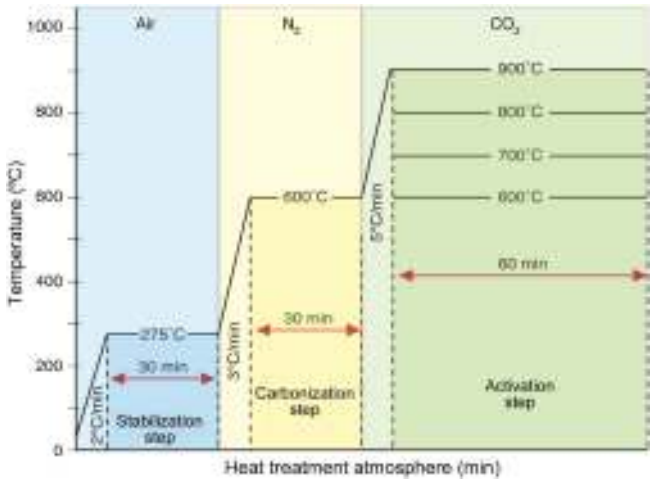

Fig. 1. Heat treatment protocol for preparation of ACFs.

The carbonization process was carried out without tension in a high-purity nitrogen stream with a flow rate of 0.2 L/min at a heating rate of 3 °C/min until 600 °C was reached. Then the temperature was kept at 600 °C for 30 min, which is known as the soaking time. The activation step of the fibers was done with the introduction of carbon dioxide gas with a flow rate of 0.2 L/min at a heating rate of 5 °C/min and at various activation temperatures of 700, 800 and 900 °C for 1 h of activation time. The fibers made at the activation temperature of 700, 800 and 900 °C are named as ACF 700, ACF 800, and ACF 900, respectively. For the case of ACF 600, the fiber is made at the 600 °C activation temperature for 1 h in the carbon dioxide gas atmosphere. It is noted that neither tension nor load was applied to the fiber during this process. The details of the heat treatment protocol can be illustrated in Figure 1.

2.3. Characterization

2.3.1. Observation of surface and surface pores by the atomic force microscopy (AFM)

The surface morphology and roughness (R_a) of the ACFs were observed by atomic force microscopy (AFM). The samples were washed in ethanol to remove all traces of glycerol. Small pieces were cut from each fiber, fixed onto magnetic disks by using double side adhesive tape and then attached to a magnetic sample holder, located on top of the scanner tube. In order to analyze the fibers internal surface, the fibers were cut longitudinally by means of a sharp razor (Hallmark Blades Ltd., Sheffield, UK). Samples intended for observation of the internal surface were sectioned on the bias so that their cylindrical shape was retained and not strained during observation.

The laser beam of the AFM was focused on a preselected spot of the surface prior to the engagement of the cantilever. AFM was operating in a tapping mode at the surface of the ACFs. Surface scanning was done at an ambient temperature under the air environment using a NanoScope III AFM equipped with a 1533D scanner (Digital Instruments, Santa Barbara, CA). The R_a was measured by visual inspection of the line profile from different areas of the carbon fiber using the NanoScope software.

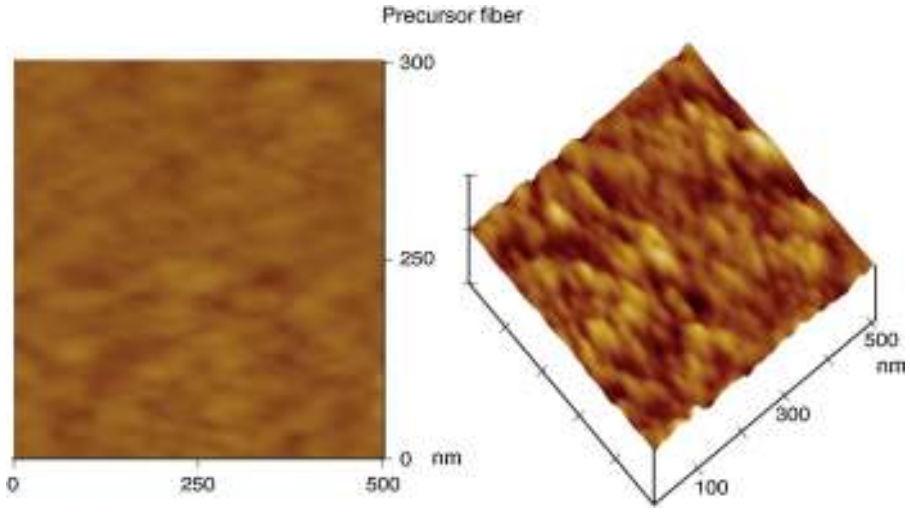

Fig. 2. AFM micrographs of the precursor fibers: 2D and 3D.

2.3.2. Fourier transform infrared (FTIR) spectroscopy

Fourier transform infrared (FTIR) spectroscopy was used to observe the presence of functional groups and chemical structure transformation of PAN/AM fibers prepared under different heat treatment stages of the fiber. The FTIR Nicolet Magna-IR 560, with potassium bromide (KBr) pellet, was used to identify and classify the chemical structure transformation of PAN/AM fibers prepared under different heat treatment stages. An IR source at 45° incident angle was employed. Both the top and bottom layer of the asymmetric fiber surface samples were mounted with facing the crystal surface. The spectra were measured at room temperature in transmittance mode over a wave number range of 4000–600 cm^{-1} at a resolution of 4 cm^{-1} and averaged over 16 scans per sample.

2.3.3. X-ray diffraction (XRD)

X-ray Diffraction (XRD) Rigaku Rint 1200 with nickel-filtered Cu Kα radiation (λ = 0.154056 nm) at 40 kV and 20 mA was performed on the PAN fibers in order to observe its crystalline related properties. The diffractogram was scanned with a scanning rate of 2° min^{-1} in a 2θ range of 5–40° at room temperature. The data was corrected for Lorentz and polarization effects, and finally normalized to a convenient standard area. The crystallinity of the samples was calculated according to this Eq. (1):

$$\text{Crystallinity} = \frac{A_c}{A_c + A_a} \times 100 \quad (1)$$

The interplanar distance (D-spacing) measurement can be obtained from the peak which appeared in the XRD pattern. The D-spacing of the fibers was calculated by the well-known Bragg equation, Eq. (2) as follows

$$\text{D-spacing} = \frac{n\lambda}{2Sin\theta} \quad (2)$$

The stacking size (Lc) was calculated by the Scherrer formula, Eq. (3):

$$\text{Lc} = \frac{k\lambda}{\beta Cos\theta} \quad (3)$$

where k is the apparatus constant (=1), λ = 0.154056 nm and β is the half-value width in the radian of X-ray diffraction intensity vs. 2θ curve.

2.3.4. X-ray photoelectron spectroscopy (XPS)

The elemental composition at the surface of the fiber was determined by X-ray photoelectron spectroscopy (XPS, Kratos Axis HS X-ray photoelectron spectrometer, Manchester, UK). Each random fiber was cut into samples of 1 cm from the carbon fiber. Monochromatized Al K_α X-radiation was used for excitation and a 180° hemispherical analyzer with a three channel detector was employed. The X-ray gun was operated at 15 kV and 20 mA. The pressure in the analyzer chamber was 1.33×10^{-4}–1.33×10^{-5} Pa. The size of the analyzed area was about 1 mm^2. All of the carbon fiber surfaces were analyzed for specific element content at a take-off angle of 0° which corresponded to the X-ray penetration depth of 6.3 nm. The angle between the normal to the sample and detector is the take-off angle (θ). At θ = 0° (i.e. sample was perpendicular to the detector), the maximum sampling depth is achieved which is 6.3 nm.

3. Results and discussion

3.1. Morphological structure properties

The fiber surface topographies of top view and 3-D images were observed using AFM. The high peaks that are seen as bright regions in the AFM images characterize the nodules, while the pores are seen as dark depressions. As shown in Figure 2, the AFM images revealed that the surfaces of the precursor fiber had nodule like structures and the nodule aggregate was formed at the surface of the fiber. As can be appreciated, there is a gradual

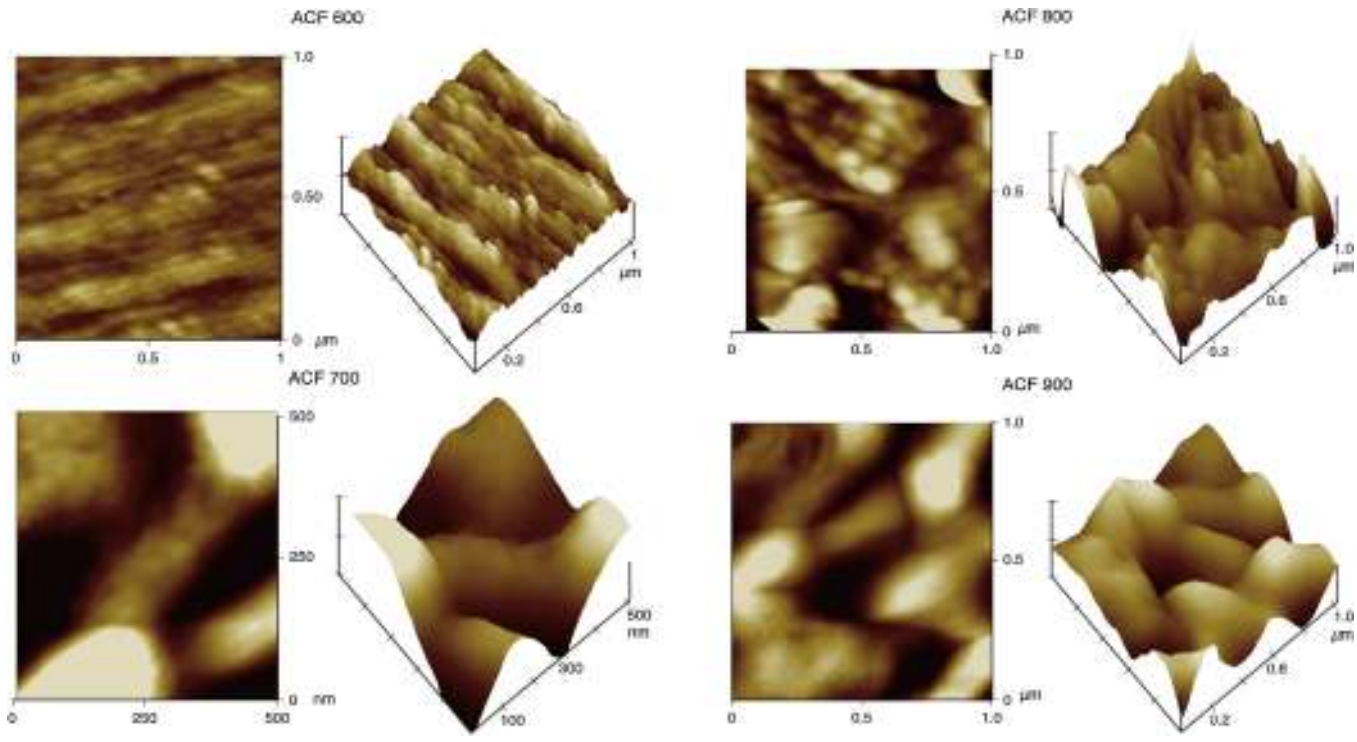

Fig. 3. AFM micrographs of the ACFs at various temperatures: 2D and 3D of ACF 600; 2D and 3D of ACF 700; 2D and 3D of ACF 800; and 2D and 3D of ACF 900.

transformation of the precursor fiber depicted in Figure 2 into the final activated carbon fiber as shown in Figure 3.

Initially, the precursor fiber presents a structure made up of long fibrils, approximately parallel to the fiber axis as a reflection of its molecular conformation shown in Figure 2. Upon the activation, the fibrils were truncated at several points, losing their long range (along the fiber axis) cohesiveness. Upon pyrolysis at 900 °C, the anisotropy of the fiber had disappeared completely and its morphology consisted of more or less rounded or elongated features arranged in a disorganized way. After activation, the characteristics of ACFs are significantly altered with the grooves and striations on the surface vanished while lots of pores emerged. The changes are mainly caused by activation (Wang et al., 2011). Similar morphological structure properties were also observed for ACFs previously studied by researchers (Wang et al., 2011; Brasquet, Rousseau, Estrade-Szwarckopf, & Le Cloirec, 2000).

The images also further indicated that the surface of the fiber becomes rougher by the increment of activation temperature as proven by the AFM images in Figure 3. In line with the physical observation, the surface roughness of ACFs was also increased after activation. Thus, referring to the data tabulated in Table 1, the mean surface roughness, R_a of the activated carbon fibers are increased from 4.16 to 13.42 nm (increment of R_a more than 3 times) with the increased activation temperature from 600 to 900 °C.

Table 1
Mean surface roughness, R_a of precursor fiber and various activated carbon fibers.

Fiber	Surface roughness, R_a (nm)
Precursor fiber	1.10
ACFs 600	4.16
ACFs 700	6.20
ACFs 800	10.08
ACFs 900	13.42

3.2. Chemical structure properties

FTIR analysis is a well known and useful method for comparing qualitatively either vibrating absorption spectra of fibers or relative intensities of the respective band (Lv, Ge, & Chen, 2009; Ryu, Rong, Zheng, Wang, & Zhang, 2002; Yusof & Ismail, 2012a). Figure 4 shows the chemical structure properties of activated carbon fibers prepared under different activation temperatures and heated in CO_2 gas stream for 60 min soaking time. There are two main broad bands in the spectra as shown in Figure 4. The band at 1220 cm^{-1} is partly associated with C–O stretching and O–H bending modes in the functional group (Ryu et al., 2002).

Meanwhile, the band in the region of 1560 cm^{-1} is assigned to an aromatic ring stretching mode or a highly conjugated hydrogen bonded C=O, analogous to the structure of acetyl acetone due to the physical activation by CO_2 gas (Figueiredo, Pereira, Fritas, & Órfão, 1999; Pradham & Sandle, 1999). As observed in Figure 4, for ACFs with higher activation temperatures (700–900 °C), it can be noticed that there is a decrease in the intensity of the bands at 1220 cm^{-1} and 1560 cm^{-1} with the increase of the activation temperature from

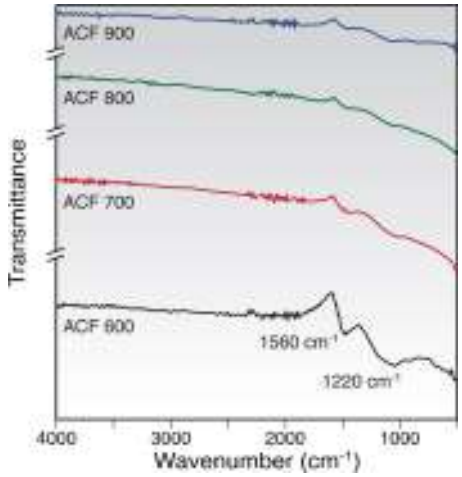

Fig. 4. FTIR spectra of the ACFs under different activation temperatures.

600 to 900 °C. All of the spectra were somewhat similar, and the main difference was the low intensity of oxygen functional groups as the activation temperature was increased to 900 °C indicating that more carbonaceous materials were formed at a higher temperature.

3.3. Microstructure properties

XRD is a useful tool for understanding the organization of carbon at the molecular level and provides qualitative and comparative assessment of the degree of packing of microstructures. The most relevant peaks when examining polymer-based carbon fibers are the (002) and (10) peaks as stated by previous researchers (Lu & Zheng, 2001; Ryu et al., 2002; Yu, Bai, Wang, Xu, & Guo, 2007). In this research, the XRD spectra for the ACFs treated at different activation temperature during activation step are shown in Figure 5. Two broad peaks at low diffraction angles are observed to correspond to the diffraction angles 2θ at 25.5–26.5° and 36–43.30°, which are assigned to the 002 plane and 10 plane (overlapped 100 and 101) of disordered micro-graphite stacking, respectively (Ryu et al., 2002; Short & Walker, 1963). The (002) peak is commonly used to determine the crystal length, which can be attributed to the turbostratic structure with randomly oriented graphitic carbon layers while the (10) peak is related to the distance between carbon atoms on the same plane (Ryu et al., 2002).

All of the ACFs samples showed wide peaks indicated the degree of amorphousness and appeared very close to the corresponding value for graphite of 0.335 nm with a diffraction peak appearing at 26.58° (Sutasinpromprae, Jitjaicham, Nithitanakul, Meechaisue, & Supaphol, 2006). It proves that the physical activation process by CO_2 gas stream toward the PAN/AM fibers prepared from the solvent-free coagulation process is a success. Concerning the plane 002, the diffraction peak appears between 2-θ degrees of 25.50–26.50° for the prepared ACFs under activation temperature of 600–900 °C, corresponding respectively to a d-spacing of around 0.3578–0.3465 nm. From the D_{002} spacing data tabulated in Table 2, it demonstrates that as the activation time increases, the graphite like layer spacing (d-spacing)

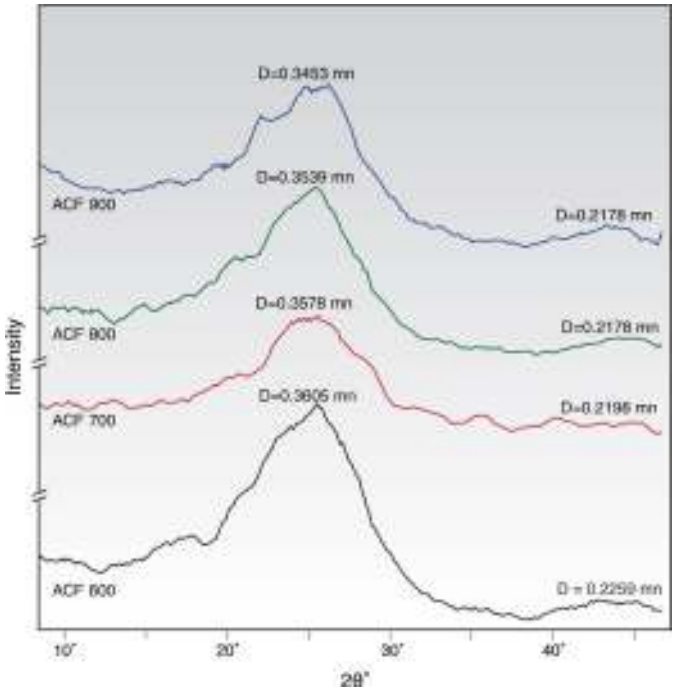

Fig. 5. XRD spectra of the ACFs under different activation temperatures. Error analysis is about ±0.01%.

of fibers declines from 0.3578 to 0.3465 nm. The decrease of the d-spacing as the activation temperature increases was also observed for ACFs prepared from physical activation previously studied by Su, Ko, and Lin (2008).

Based on XRD spectra on the ACFs prepared at different activation conditions, it can be concluded that the graphite sheets have been constructed in carbon structure during the activation step. The activation of the ACFs shrank the ordered structure, reducing the d-spacing from, 0.358 to 0.347 nm, which corresponds to 3.5% contraction, for the fibers prepared at activation temperature of 600–900 °C. Meanwhile, another peak correlated to the graphite (10) plane, D_{10} spacing, represents the repeated aromatic ring in the graphitic structure between $2\theta = 43–45.5°$ was observed in all samples of the activated carbon fibers as tabulated in Table 2.

Referring to the crystallite size data in Table 2, all of the ACFs samples prepared contain disordered graphite micro-crystallites, with inter-crystallite and intra-crystallite voids forming the pores with the crystallite size of ACFs ranging from 1.286 to 2.916 nm. From the XRD results, the crystal size decreases with the increase of the activation temperature. Similar findings were reported by previous researchers (Lu & Zheng, 2001; Ryu et al.,

Table 2
Structural parameters of precursor fiber and various activated carbon fibers.

Fiber	Spacing D_{002} (nm)	Spacing D_{10} (nm)	Crystallite size, Lc (nm)
ACFs 600	0.358	0.226	2.591
ACFs 700	0.360	0.220	2.916
ACFs 800	0.354	0.218	1.565
ACFs 900	0.345	0.218	1.286

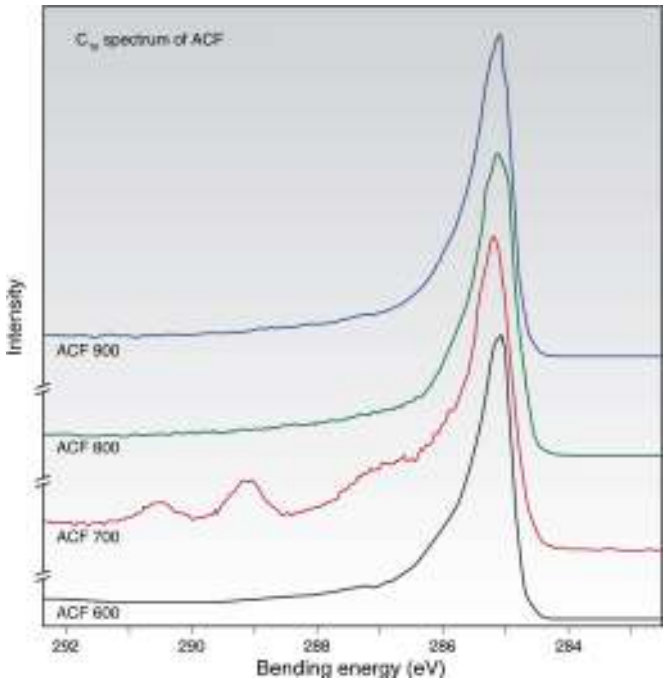

Fig. 6. C_{1S} spectra of the ACFs under different activation temperatures.

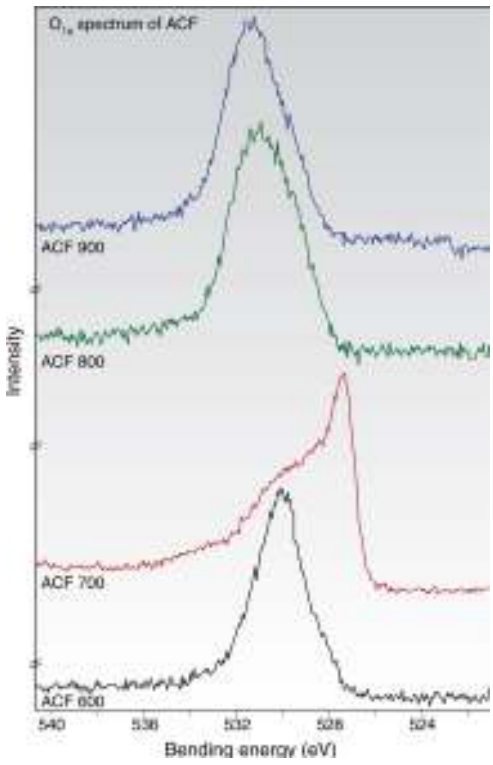

Fig. 7. O_{1S} spectra of the ACFs under different activation temperatures.

2002). ACF 900 has the smallest crystallite size (1.286 nm) and the shortest D_{002} spacing was observed at 0.345 nm. A small crystallite size and short range ordering between crystallites provides the prerequisites for the realization of high surface area activated carbon fibers (Ryu et al., 2002). Thus, a short conclusion can be made that 900 °C is the optimum activation temperature for the production of high performance adsorbent media.

Meanwhile, the chemical composition and binding characteristic at the surface of the fiber was determined by X-ray photoelectron spectroscopy investigation. The X-ray photoelectron spectroscopy spectra of the ACFs samples contain three distinct major peaks due to carbon, nitrogen and oxygen. In order to clarify the functionalities and their variation with the activation temperature, curve fitting procedures on the C_{1S}, O_{1S} and N_{1S} spectra were investigated. Referring to Figure 6(a–d), it can be concluded that all of the prepared ACFs samples show an asymmetrical shape for the C_{1S} spectra extending from 283 to 288 eV.

This chemical shift toward higher binding energies indicates that there are various carbon-based functional groups on the surface of these ACFs. A major peak at 284 ± 0.5 eV is attributed to C–C/C–H of carbidic/graphitic carbon (Biniak, Szymański, Siedlewski, & Świątkowski, 1997; Jansen & van Bekum, 1995). In addition, a series of chemically shifted peaks is observed at the high-binding energy side. Several minor peaks are generally observed, which occur at binding energies at about 286 ± 0.5 eV, 287 ± 0.5 eV and 289 ± 0.5 eV, respectively. They can be assigned to C–O (ether/hydroxyl) and/or C–N, C=O (carbonyl), and O–C=O (carboxyl) functionalities respectively appeared upon the heat treatment (Biniak et al., 1997; Wang, Hong, & Zhu, 1996).

The typical O_{1S} spectra in Figure 7(a–d) appear to contain mainly three chemically shifted peaks. The main peak at a binding energy of about 531 ± 0.5 eV is attributed to C=O groups (ketone, lactone, carbonyl). While the peak at 533 ± 0.5 eV is probably due to C–O in esters, amides, carboxylic anhydrides and oxygen atoms in hydroxyls or ethers, while the other peak at 535 ± 0.5 eV is tentatively assigned to chemisorbed oxygen and/or water. Thus, based on the C_{1S} and O_{1S} spectrum analyses, it can be interfered that there are several forms of carbon-oxygen functionalities present on the surface of the fiber.

Meanwhile, the N_{1S} spectra in Figure 8(a–d) indicates that not only does nitrogen exist in various functionalities on the surfaces, but these nitrogen functionalities vary to some extent from activation temperature of 600–900 °C (Wang et al., 1996). The N_{1S} spectra contain two major chemically shifted peaks: isonitriles compound (398 ± 0.5 eV) and aromatic amine (399 ± 0.5 eV) (Ryu et al., 2002). Other assignments of peaks 399.0–400.0 eV could be attributed to amide functionality due to the addition of acrylamide in the precursor PAN/AM fibers, and the peak at 400–401 eV were credited to aliphatic amine, while the peak around 400.9–401.7 eV was probably due to protonated primary amine ($-NH_3^+$) (Wang et al., 1996). From the N_{1S} spectra, it can also be observed that the intensity of the lower binding energy peak gradually decreased when subjected to the higher activation temperature. This suggested that the elimination of aromatic amine occurred during these heat treatment activities.

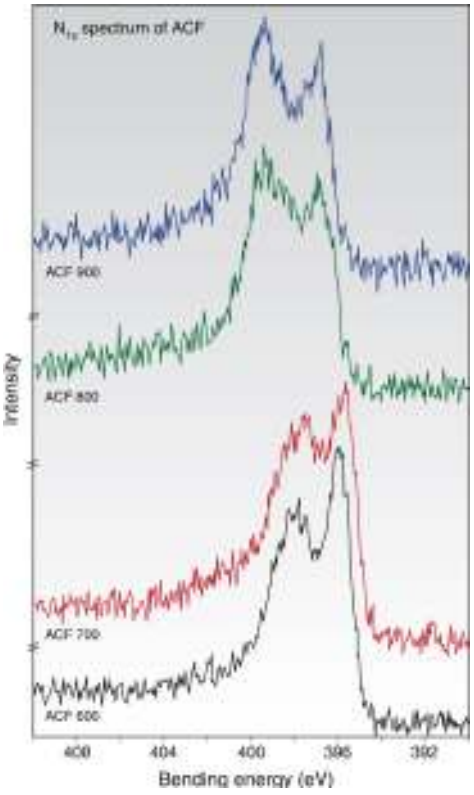

Fig. 8. N_{1S} spectra of the ACFs under different activation temperatures.

4. Conclusions

The AFM micrographs analysis shows that porosity is increased together with the loss of volatile components through the activation process. Meanwhile, the success of physical activation of carbonized AM/PAN fiber using CO_2 gas at 900 °C is proved by FTIR, XRD, and XPS analysis. The intensity of oxygen functional groups is lowered as the activation temperature was increased to 900 °C indicating that more carbonaceous materials were formed at a higher temperature. The activation of the ACFs shrank the ordered structure, reducing the d-spacing from, 0.358 to 0.347 nm with an increase of temperature. Thus, based on the C_{1S} and O_{1S} spectrum analyses, it can be interfered that there are several forms of carbon-oxygen functionalities present on the surface of the fiber. The N1s results suggested that the elimination of aromatic amine occurred during these heat treatment activities. These observations infer that nitrogen originating from PAN, AM and DMF decreases but oxygen containing functional groups remain, while hollow fiber is heated in CO_2 atmosphere. In the meantime, d-spacing decreases leading to more compact structure. It is also proved that the precursor fibers prepared via environmental friendly solvent-free coagulation processes that the micro-porous structure confirmed its potential to be used as an adsorbent media for gas separation in the near future.

Conflict of interest

The authors have no conflicts of interest to declare.

Acknowledgment

The authors would like to acknowledge the financial support from Universiti Teknologi Malaysia under Grant Q.J130000.2542.05H46 and Q.J130000.2546.12H54. The authors would also like to acknowledge the technical and management support from Research Management Centre (RMC), Universiti Teknologi Malaysia.

References

Biniak, S., Szymański, G., Siedlewski, L., & Świątkowski, A. (1997). The characterization of activated carbons with oxygen and nitrogen surface groups. *Carbon*, *35*(12), 1799–1810. http://dx.doi.org/10.1016/S0008-6223(97)00096-1

Brasquet, C., Rousseau, B., Estrade-Szwarckopf, H., & Le Cloirec, P. (2000). Observation of activated carbon fibres with SEM and AFM correlation with adsorption data in aqueous solution. *Carbon*, *38*(3), 407–422. http://dx.doi.org/10.1016/S0008-6223(99)00120-7

Chiang, Y. C., Lee, C.-C., & Lee, H.-C. (2007). Characterization of microstructure and surface properties of heat-treated PAN-and rayon-based activated carbon fibers. *Journal of Porous Material*, *14*(2), 227–237. http://dx.doi.org/10.1007/s10934-006-9028-8

Figueiredo, J. L., Pereira, M. F. R., Fritas, M. M. A., & Órfão, J. J. M. (1999). Modification of the surface chemistry of activated carbons. *Carbon*, *37*(9), 1379–1389. http://dx.doi.org/10.1016/S0008-6223(98)00333-9

Ismail, A. F., Rahman, M. A., Mustafa, A., & Matsuura, T. (2008). The effect of processing conditions on a polyacrylonitrile fiber produced using a solvent-free free coagulation process. *Materials Science and Engineering: A*, *485*(1–2), 251–257. http://dx.doi.org/10.1016/j.msea.2007.08.060

Jansen, R. J. J., & van Bekum, H. (1995). XPS of nitrogen-containing functional groups on activated carbon. *Carbon*, *33*(8), 1021–1027. http://dx.doi.org/10.1016/0008-6223(95)00030-H

Lu, A.-H., & Zheng, J.-T. (2001). Study of microstructure of high-surface-area polyacrylonitrile activated carbon fibers. *Journal of Colloid and Interface Science*, *236*(2), 369–374. http://dx.doi.org/10.1006/jcis.2000.7425

Lv, M.-Y., Ge, H.-Y., & Chen, J. (2009). Study on the chemical structure and skin-core structure of polyacrylonitrile-based fibers during stabilization. *Journal of Polymer Research*, *16*(5), 513–517. http://dx.doi.org/10.1007/s10965-008-9254-7

Pradham, B. K., & Sandle, N. K. (1999). Effect of different oxidizing agent treatments on the surface properties of activated carbons. *Carbon*, *37*(8), 1322–1332. http://dx.doi.org/10.1016/S0008-6223(98)00328-5

Ryu, Z., Rong, H., Zheng, J., Wang, M., & Zhang, B. (2002). Microstructure and chemical analysis of PAN-based activated carbon fibers prepared by different activation methods. *Carbon*, *40*(7), 1144–1147. http://dx.doi.org/10.1016/S0008-6223(02)00105-7

Sedghi, A., Farsani, R. E., & Shokuhfar, A. (2008). The effect of commercial polyacrylonitrile fibers characterization on the produced carbon fiber properties. *Journal of Materials Processing Technology*, *198*(1–3), 60–67. http://dx.doi.org/10.1016/j.jmatprotec.2007.06.052

Short, M. A., & Walker, P. L., Jr. (1963). Measurement of interlayer spacing and crystal sizes in turbostratic carbons. *Carbon*, *1*(1), 3–9. http://dx.doi.org/10.1016/0008-6223(63)90003-4

Su, Y.-J., Ko, T.-H., & Lin, J.-H. (2008). Preparation of ultra-thin PAN-based activated carbon fibers with physical activation. *Journal of Applied Polymer Science*, *108*(6), 3610–3617. http://dx.doi.org/10.1002/app.27982

Sutasinpromprae, J., Jitjaicham, S., Nithitanakul, M., Meechaisue, C., & Supaphol, P. (2006). Preparation and characterization of ultrafine electrospun polyacrylonitrile fibers and their subsequent pyrolysis to carbon fibers. *Polymer International*, *55*(8), 825–833. http://dx.doi.org/10.1002/pi.2040

Tsai, J.-S. (1994). Coefficient variation of the mechanical properties of carbon fiber during carbonization. *Journal of Polymer Research*, *1*(4), 399–402. http://dx.doi.org/10.1007/BF01378774

Wang, P. H., Hong, K. L., & Zhu, Q. R. (1996). Surface analyses of polyacrylonitrile-based activated carbon fibers by X-ray photoelectron

spectroscopy. *Journal of Applied Polymer Science*, *62*(12), 1987–1991. http://dx.doi.org/10.1002/(SICI)10974628(19961219)62:12<1987::AID-APP2>3.0.CO;2-E

Wang, G., Han, H., Li, L., Quan, H., Shi, Y., Qin, W., et al. (2011). SEM and AFM studies on the surface and cross section morphology of rayon based activated carbon fiber. *Materials Science Forum*, *689*, 413–418. http://dx.doi.org/10.4028/www.scientific.net/MSF.689.413

Yusof, N., & Ismail, A. F. (2012). Polyacrylonitrile/acrylamide-based carbon fibers prepared using a solvent-free coagulation process: Fiber properties and its structure evolution during stabilization and carbonization. *Polymer Engineering & Science*, *52*(2), 360–366. http://dx.doi.org/10.1002/pen.22090

Yu, M.-J., Bai, Y.-J., Wang, C.-G., Xu, Y., & Guo, P.-Z. (2007). A new method for the evaluation of stabilization index of polyacrylonitrile fibers. *Materials Letters*, *61*(11–12), 2292–2294. http://dx.doi.org/10.1016/j.matlet.2006.08.071

Yusof, N., & Ismail, A. F. (2012). Post spinning and pyrolysis processes of polyacrylonitrile (PAN)-based carbon fiber and activated carbon fiber: A review. *Journal of Analytical and Applied Pyrolysis*, *93*, 1–13. http://dx.doi.org/10.1016/j.jaap.2011.10.001

Yusof, N., Ismail, A. F., Rana, D., & Matsuura, T. (2012). Effects of the activation temperature on the polyacrylonitrile/acrylamide-based activated carbon fibers. *Materials Letters*, *82*, 16–18. http://dx.doi.org/10.1016/j.matlet.2012.04.150

Zhao, N., He, C., Jiang, Z., Li, J., & Li, Y. (2007). Physical activation and characterization of multi-walled carbon nanotubes catalytically synthesized from methane. *Materials Letters*, *61*(3), 681–685. http://dx.doi.org/10.1016/j.matlet.2006.05.041